

Observation of film states and surface-state precursors for Ag films on Si(111)

A. L. Wachs, A. P. Shapiro, T. C. Hsieh, and T.-C. Chiang

*Department of Physics and Materials Research Laboratory,
University of Illinois, Urbana, Illinois 61801*

(Received 30 September 1985; revised manuscript received 11 November 1985)

Ag films on Si(111)-(7×7) having thicknesses of 0–17 monolayers were studied with angle-resolved photoemission. The spectra exhibit quasiperiodic peaks with separations between neighboring peaks approximately proportional to the inverse of the film thickness. These are film states associated with the *sp* band of bulk Ag. A surface-state precursor was also observed on films as thin as two monolayers in thickness.

The restricted geometry in thin films may lead to significant modifications in their electronic properties as compared to those of the corresponding bulk crystal. In this paper, we report the observation, using angle-resolved photoemission, of film states derived from the *sp* band of bulk Ag for thin Ag films prepared on Si(111)-(7×7) at room temperature. The film states appear in the normal-emission spectra as quasiperiodic peaks with energy separations between neighboring peaks approximately proportional to the inverse of the film thickness. We have also observed the precursor of a surface state for Ag films as thin as two monolayers (ML) in thickness.

The quantum size effects associated with thin films have been observed before. For example, in thin-film tunneling experiments at low temperatures, the tunneling current can exhibit oscillations as a function of the bias voltage.¹ The oscillations are explicable in terms of “commensurate states” near specific points in the Brillouin zone. The photoluminescence or lasing wavelengths of certain epitaxially grown semiconductor superlattices can show a blue shift upon reduction of the active layer thickness.² This shift in optical transition energy has been explained simply in terms of the extra energy associated with a particle confined in a small one-dimensional box.

The present experiment differs in several important aspects from these earlier works. The thicknesses of our samples, 0–17 ML (0–40 Å) are significantly smaller than those used in tunneling experiments (> 100 Å) and in photoluminescence experiments (> 50 Å). Surface and interface effects are therefore much more important. In the present experiment, the occupied states are independently probed, as opposed to the transition energies between electron and hole states in the photoluminescence measurements. The tunneling measurements had to be performed at low temperatures to avoid thermal broadening effects. Our experiment was performed at room temperature; the thermal broadening effects are not as important because the very-thin-film states have relatively large energy separations.

The fact that well-resolved peaks derived from thin-film states were observed indicates that our Ag-film samples had a fairly uniform thickness. This result has important implications concerning the growth mode of Ag on Si(111)—a subject of considerable interest and controversy in recent years.^{3,4}

The photoemission measurements were performed at the Synchrotron Radiation Center of the University of Wisconsin at Madison. Synchrotron radiation from the 240-MeV Tantalus storage ring was monochromatized by either the

Mark-V monochromator or a Seya monochromator. The photoemitted electrons in the sample-normal direction were analyzed with a hemispherical analyzer having an acceptance full angle of 3° and detected by pulse counting. The procedure for preparation of the Si(111)-(7×7) substrates and the subsequent deposition of Ag overlayers at room temperature have been described elsewhere.⁴ A single-crystal Ag(111) sample was prepared by sputtering and annealing in the usual manner. The overlayer growth mode, morphology, and epitaxial relationship of Ag on Si were examined with high-energy electron diffraction (HEED), Auger spectroscopy, and core-level photoemission from the substrate. We determined that the Ag films prepared at room temperature were fairly smooth and exhibited a domained structure in a predominantly parallel epitaxy configuration (i.e., the crystallographic axes of the overlayer are parallel to those of the substrate) with little distortion in both the Ag and Si lattice parameters.⁴ The Auger and core-level measurements showed that the films were slightly leaky, implying that there might be a small portion of the substrate surface covered by substantially less than the average Ag thickness.

Figure 1 shows a set of normal-emission spectra taken with a photon energy of 22 eV from clean Si(111)-(7×7), Si(111) covered by various thicknesses of Ag, and a single-crystal Ag(111) sample. The spectra as presented were obtained from the sum of multiple scans followed by three-point averaging. The many small noise spikes are derived from statistical fluctuations, and can be easily distinguished from true spectral features by the fact that they are much narrower than the instrumental resolution of about 0.2 eV. The bottom spectrum in Fig. 1, taken from clean Si(111)-(7×7), shows three surface-state-derived features with binding energies (E_B) at about 0.3, 0.9, and 1.8 eV and a smooth background due to bulk emission.⁵ With an Ag coverage equivalent to an average overlayer thickness of $T=0.75$ ML, the (7×7) reconstruction is suppressed, and the two surface-state features near E_F are nearly completely quenched, as seen in Fig. 1. For $T=2$ ML, a new feature, indicated by a short bar in Fig. 1, appears in the spectrum close to E_F . This feature evolves continuously, sharpening up as T increases, and finally settles at an energy position just below E_F . This peak is also present in the spectrum for clean Ag(111) shown in Fig. 1, and is associated with an Ag(111) surface state (see below).^{6,7}

In the spectra for $T=5$ –15 ML in Fig. 1, many relatively weak features, indicated by circles and triangles, can be seen by careful visual inspection (especially with grazing viewing angles). These features are readily verified to be associated

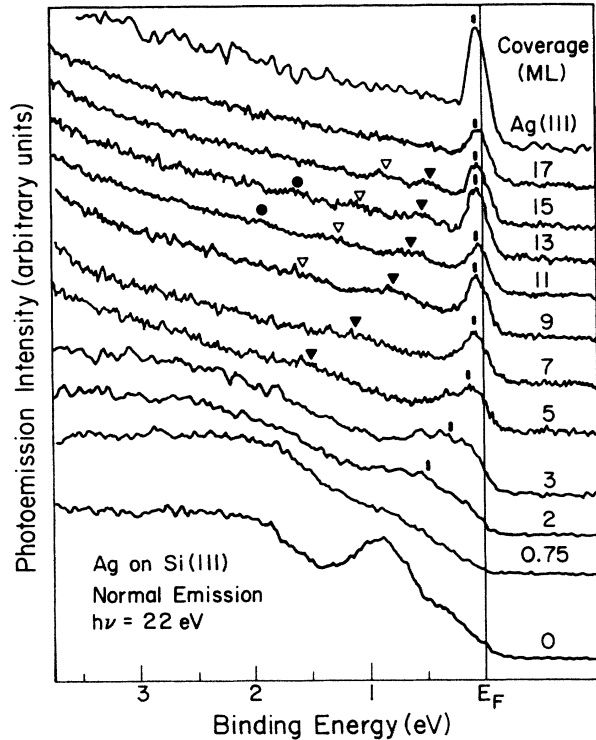


FIG. 1. Photoemission spectra taken with a normal-emission geometry and a photon energy $h\nu=22$ eV from clean Si(111)- (7×7) (bottom spectrum), Si(111) covered with various thicknesses of Ag as indicated, and a single-crystal Ag(111) sample (top spectrum). The short bars, triangles (filled and open), and filled circles indicate peak positions. The binding-energy scale is referred to the Fermi level E_F .

with the film states, as they evolve continuously with changing T . For a better presentation of the results, each of these spectra was digitally processed by low-pass filtering of the Fourier transform of the spectrum with a Gaussian window function centered about zero (in much the same way as is typically done in the extended x-ray absorption fine-structure analysis). The inverse Fourier transform of the Gaussian window function is itself a Gaussian function of full width at half maximum (FWHM) of 0.2–0.45 eV; the smaller values were used for the cases with better signal-to-noise ratios. Real spectral features in the region of interest are expected to have a FWHM about equal to or larger than the largest FWHM of the Gaussian filtering functions used. The factors contributing to the spectral width include instrumental broadening (0.2 eV), lifetime broadening (≥ 0.3 eV, depending on the initial energy),^{8,9} inhomogeneous broadening due to film-thickness fluctuation (~ 1 ML), and the incommensurate interface potential, etc. Thus, the filtering preferentially suppresses statistical noise features that exhibit rapid random fluctuations, while the real spectral features are not affected much. After filtering, a somewhat arbitrary smooth cubic polynomial background function is subtracted from each spectrum to get rid of the steep background for as wide an energy range as possible. The results are shown in Fig. 2 as solid curves with a greatly magnified vertical scale. The weak features indicated in Fig. 1 now appear as well-defined peaks in Fig. 2; in addition, a few even weaker peaks become noticeable. The noise is not totally eliminated by the digital processing, however; there-

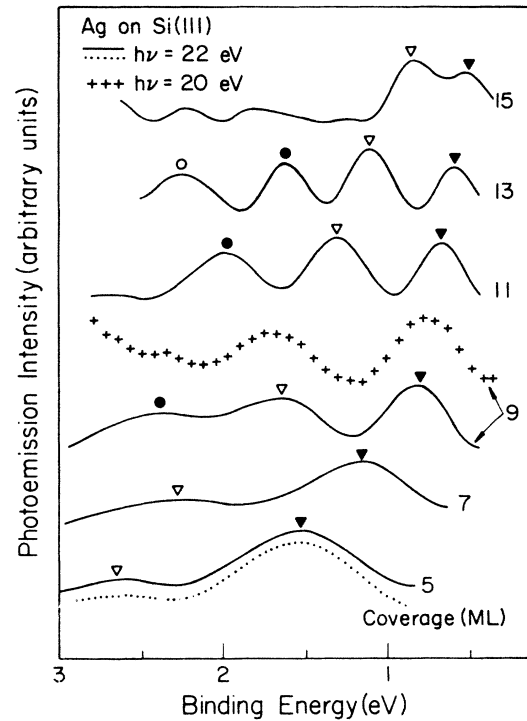


FIG. 2. The solid curves are portions of the spectra shown in Fig. 1 obtained after digital filtering and background subtraction. Spectral peaks are indicated by triangles and circles. The crosses represent a spectrum obtained with $h\nu=20$ eV; the dotted curve shows a spectrum obtained from a different sample. The Ag coverages are as indicated.

fore, extremely weak peaks (with a small net area under the curve) are ignored in the analysis. Note that these peaks have heights only about $\frac{1}{300}$ of the Ag 4d peak heights. The peaks are probably also present in the spectra for $T=17$ ML and $T\leq 3$ ML in Fig. 1, but are too indistinct for positive identification. To demonstrate reproducibility, a spectrum obtained from a different Si sample covered by 5 ML of Ag is shown by the dotted curve in Fig. 2 for comparison. Data taken with other photon energies, including 14, 16, 18, and 20 eV, also show these peaks at the same binding energies. For example, the curve shown by the crosses in Fig. 2 for 9-ML Ag coverage was obtained using 20-eV photons and exhibits peaks at the same energies.

Figure 3 shows the band structure of bulk Ag for the wave vector k along the L - Λ - Γ or $\langle 111 \rangle$ direction;^{7,10} this is the direction probed by the normal-emission geometry. The abscissa is measured in units of $\pi\sqrt{3}/a$, the distance between L and Γ (a is the lattice parameter). The Ag 4d bands, shown schematically by the hatched area in Fig. 3, extend roughly from $E_B=4$ –7 eV; they give rise to intense photoemission peaks (results not shown here).⁴ Between the top of the 4d bands and E_F , there is only one band, the free-electron-like sp band. The upper edge of this band is at the L point; a surface state lies just slightly above this edge as indicated in Fig. 3. This surface state gives rise to the sharp peak near E_F in Fig. 1 for clean Ag(111).⁶⁻⁸

The Ag(111) surface state has a probability-density decay length equivalent to 6 ML.⁷ Thus it is reasonable for Ag films with $T\geq 6$ ML to support a similar state with nearly

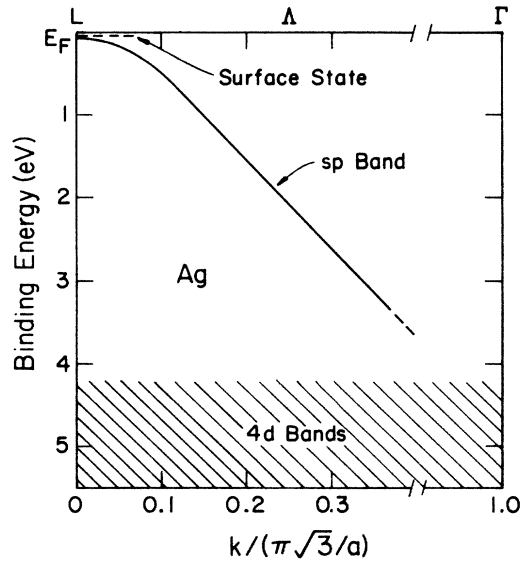


FIG. 3. Schematic band structure of Ag for k (wave vector) along the $\langle 111 \rangle$ direction measured from the L point to the Γ point in units of $\pi\sqrt{3}/a$ (distance between L and Γ). The energy position of the surface state on Ag(111) is indicated by a horizontal dashed line.

the same binding energy as that of the single-crystal Ag(111) sample. This is indeed observed in Fig. 1. As the Ag film gets thinner, the perturbation of the Ag-Si interface upon the surface state becomes more important and thus the binding-energy shift becomes larger. For small T , the wave function no longer has pure surface-state character;⁷ it is therefore appropriate to call the small- T states surface-state precursors.

We now consider the behavior of the sp band states as the film thickness T becomes small. Periodic boundary conditions that give a good description of the bulk properties for large T lead to a set of Bloch states $\psi(r;k)$ for k along $\langle 111 \rangle$. The allowed values of k are $2n\pi/T$, where $n=0, \pm 1, \pm 2, \dots$. The two states $\psi(r;k)$ and $\psi(r;-k)$ are degenerate; hence, the allowed values of k can be restricted to non-negative values only, with the understanding that each positive value of k corresponds to two degenerate states. If, instead, the boundary conditions are those for a box with infinite walls, the allowed values of k become $n\pi/T$, where $n=1, 2, 3, \dots$.¹ For Ag films on Si, the real boundary conditions resemble neither of the two above-mentioned cases exactly,¹¹ and

$$k = (n + \delta)\pi/T, \quad (1)$$

where $n=0, 1, 2, \dots$. δ , the quantum defect, is related to the phase shift and depends on n and T ; it is real with $|\delta| < 1$ for $n > 0$. k can be imaginary if $n=0$; this corresponds to the surface state for large T .^{7,12} Clearly, the allowed values of k become sparse as T becomes small; the total number of states is just the number of layers in the film. Over the energy range where the film states are observed ($E_B \approx 0.5\text{--}3$ eV), the sp band shown in Fig. 3 has roughly a constant group velocity v . Therefore, the binding energies of the film states derived from the sp band are

$$E_B(n;t) \approx E_0 - (n + \delta)\pi\hbar v/T, \quad (2)$$

where E_0 is a constant. Since δ , being a phase-shift factor, is expected to be a smooth function of E_B and T , the film states for a given T should be roughly equally spaced in energy for increasing n . Also, the energy spacing between neighboring film states differing in n by one should be roughly proportional to T^{-1} according to Eq. (2). In fact, the energy spacing should be approximately given by the sp -band width (about 7 eV ignoring the mixing with the $4d$ states)¹⁰ divided by the number of layers. The readers can easily verify these points qualitatively by visually inspecting the spectra.

Based on the above arguments, it is evident that the peaks indicated in Fig. 2 are indeed film states derived from the sp band for bulk Ag. We now analyze the data in a more quantitative manner. The values of k measured from L to Γ for all the peaks seen in Figs. 1 and 2 have been determined by using their experimental binding energies in conjunction with Fig. 3. The surface-state-derived peak has a small imaginary value of k if its energy position lies above the sp -band edge.^{7,12} We shall ignore this small imaginary component in our discussion. The values of k multiplied by T/π are shown in Fig. 4 for the different peaks as a function of T . According to Eq. (1),

$$kT/\pi = n + \delta. \quad (3)$$

Clearly, the five peaks observed in Figs. 1 and 2 can be associated with $n=0, 1, 2, 3$, and 4, respectively, with $n=0$ corresponding to the surface-state precursor. The quantum defect δ for different n as a function of T can then be easily obtained from Fig. 4. It can be used, in principle, to deduce the surface and interface potentials. No theoretical or other experimental values of δ exist in the literature as far as we know.

In summary, we have observed film states and the precursor of a surface state in Ag films on Si(111). The

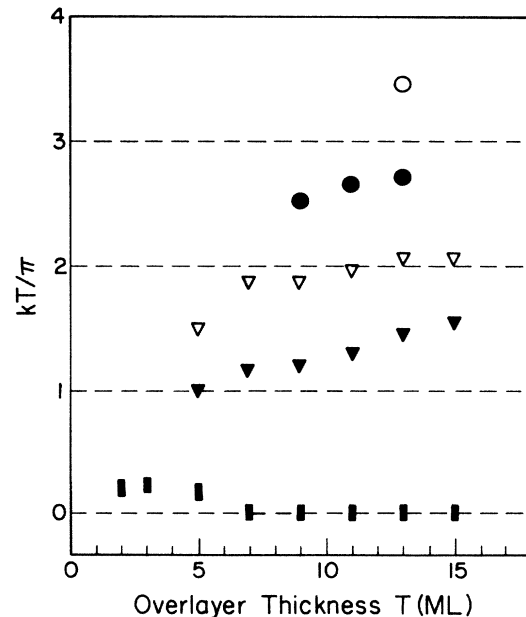


FIG. 4. Values of kT/π plotted as a function of the overlayer thickness T for the peaks seen in Fig. 1. The symbols for the data points correspond to those used in Figs. 1 and 2 to indicate the peak positions.

surface-state precursor has even been observed for films as thin as 2 ML; in this case, its wave function must be quite dissimilar to that of the surface state of bulk Ag(111). The frequently raised question regarding the critical film thickness for supporting a surface state¹³ has no well-defined meaning for the present system; just imagine, for example, the limiting case that $T = 1$ ML, for which there is only one state associated with the sp band. The intensities of the film states ($n = 1-4$) are weak in our spectra. This is perhaps not surprising, since the sp band leads to only weak emission intensities via indirect transitions for bulk Ag(111) under our experimental conditions.⁸

The fact that well-resolved peaks are observed in Figs. 1 and 2 indicates that the film thickness of our samples has a fairly sharp distribution. For example, the $n = 1$ peak for $T = 7$ ML is almost at the same energy as that for the valley between the $n = 1$ and $n = 2$ peaks for $T = 9$ ML. If the $T = 9$ -ML film had a thickness distribution wider than about ± 2 ML, the structures in the spectra would be essentially smeared out. The Ag films are not perfect, however, as dis-

cussed above; the presence of thin spots may be related to imperfections in the substrate, the nonequilibrium nature of the growth process, and/or the domained structure of the overlayer (the domain boundaries may be leaky). The imperfection in the film structure probably also explains the fact that the surface-state photoemission peak from thick Ag films on Si(111) is never as intense as the one from our single-crystal Ag(111) sample (see Fig. 1).¹⁴

This material is based upon work supported by the U. S. Department of Energy, Division of Materials Sciences, under Contract No. DE-AC02-76ER01198. Some of the equipment used for this research was obtained with grants from the National Science Foundation (Grant No. DCR-8352083), the IBM Research Center, the Research Corporation, and the General Motors Research Laboratories. We are grateful to the staff of the Synchrotron Radiation Center of the University of Wisconsin for assistance. The Synchrotron Radiation Center is supported by the National Science Foundation under Contract No. DMR-8020164.

¹R. C. Jaklevic and J. Lambe, *Phys. Rev. B* **12**, 4146 (1975).

²R. M. Kolbas and N. Holonyak, *Am. J. Phys.* **52**, 431 (1984).

³G. LeLay, M. Manneville, and R. Kern, *Surf. Sci.* **72**, 405 (1978); M. Hanbucken, H. Neddermeyer, and P. Rupieper, *Thin Solid Films* **90**, 37 (1982); G. Dufour, J.-M. Mariot, A. Masson, and H. Roulet, *J. Phys. C* **14**, 2539 (1981); F. Houzay *et al.*, *Surf. Sci.* **124**, L1 (1983); Y. Gotoh and S. Ino, *Jpn. J. Appl. Phys.* **17**, 2097 (1978); M. Hanbucken, M. Futamoto, and J. A. Venables, in *Electron Microscopy and Analysis*, The Institute of Physics Conference Proceedings No. 68, edited by P. Doig (The Institute of Physics, Bristol, 1984), pp. 135-138; E. J. van Loenen, M. Iwami, R. M. Tromp, and J. F. van der Veen, *Surf. Sci.* **137**, 1 (1984).

⁴A. L. Wachs, T. Miller, and T.-C. Chiang, *Phys. Rev. B* **29**, 2286 (1984).

⁵A. L. Wachs, T. Miller, T. C. Hsieh, A. P. Shapiro, and T.-C. Chiang, *Phys. Rev. B* **32**, 2326 (1985).

⁶P. Heimann, H. Neddermeyer, and H. F. Rologg, *J. Phys. C* **10**, L17 (1977).

⁷T. C. Hsieh, A. P. Shapiro, and T.-C. Chiang, *Phys. Rev. Lett.* **55**, 2483 (1985); *Surf. Sci.* (to be published); and unpublished results.

⁸P. S. Wehner *et al.*, *Phys. Rev. B* **19**, 6164 (1979).

⁹J. A. Knapp, F. J. Himpsel, and D. E. Eastman, *Phys. Rev. B* **19**, 4952 (1979).

¹⁰N. E. Christensen, *Phys. Status Solidi (b)* **54**, 551 (1972); H. Eckardt, L. Fritsche, and J. Noffke, *J. Phys. F* **14**, 97 (1984); V. L. Moruzzi, J. F. Janak, and A. R. Williams, *Calculated Electronic Properties of Metals* (Pergamon, New York, 1978), p. 148. These different theoretical calculations give slightly different bulk band dispersions; therefore, the dispersion of the sp band is slightly uncertain. The part of the sp -band dispersion very near E_F shown in Fig. 3 is taken from Ref. 7.

¹¹See, for example, L. I. Schiff, *Quantum Mechanics*, 3rd ed. (McGraw-Hill, New York, 1968), pp. 37-44.

¹²See, for example, N. W. Ashcroft and N. D. Mermin, *Solid State Physics* (Saunders College, Philadelphia, 1976), pp. 367-371.

¹³S.-L. Weng and M. El-Batanouny, *Phys. Rev. Lett.* **44**, 612 (1980).

¹⁴However, the surface-state photoemission peaks from thick Ag films seen in Fig. 1 show comparable or better peak-to-background ratios when compared with some earlier published works on single-crystal Ag(111) samples under similar experimental conditions.